

UDC 621.744.3

DOI <https://doi.org/10.32782/3041-2080/2026-7-13>

## THE INFLUENCE OF MOLD TYPE ON SURFACE QUALITY PARAMETERS AND STRUCTURE IN THE PRODUCTION OF ARTISTIC CASTINGS USING PATTERNS OBTAINED BY ADDITIVE METHODS

**Gnatenko Mykhailo Olehovych,**

Doctor of Philosophy,

Senior Lecturer at the Department of Machines and Technology of Foundry Production

National University «Zaporizhzhia Polytechnic»

ORCID ID: 0000-0002-7613-852X

**Matveishyn Mykyta Vitaliovych,**

Senior Lecturer at the Department of Machines and Technology of Foundry Production

National University «Zaporizhzhia Polytechnic»

ORCID ID: 0000-0001-6050-310X

**Serhiienko Olha Serhiiivna,**

Associate Professor at the Department of Machines and Technology of Foundry Production

National University «Zaporizhzhia Polytechnic»

ORCID ID: 0000-0001-5575-9856

**Ivanov Valery Hryhorovych,**

Head of the Department of Machines and Technology of Foundry Production

National University «Zaporizhzhia Polytechnic»

ORCID ID: 0000-0002-9216-3493

*Purpose.* To investigate the influence of different molding materials on the surface quality and structural characteristics of bronze castings, and to evaluate the technological advantages of combining additive manufacturing (with investment casting for producing bronze artworks).

*Research Methods. Technologies Compared:* The study investigated casting methods: Lost-PLA Plaster (IC), no-bake molds (NB), and sand-clay molds (SC).

*Master Model:* A 3D-printed PLA master model was used. For NB and SC molds, a non-destructive model was used, while for IC, the PLA was removed during thermal burnout process (700 °C for one hour).

*Design Parameters:* The model design incorporated specific casting parameters: draft angles of 2°, minimum wall thicknesses of 2 mm, and machining allowances of 1 mm.

*Analysis:* The study analyzed surface roughness (Ra and Rz), grain size, porosity, and mold cooling rates.

*Results. Surface Quality:* Lost-PLA Plaster Investment casting (IC) produced the best results with the lowest surface roughness (Ra = 2.8 μm, Rz = 12.5 μm), highest relief fidelity, absence of gas porosity, and minimal burn-on. No-bake (NB) molds showed intermediate quality, and sand-clay (SC) molds had the poorest indicators. *Microstructure:* Grain size analysis matched the surface quality trend. IC produced the finest microstructure (25.3 μm), followed by NB (25.5 μm) and SC (27.8 μm).

*Cooling Rates:* The grain size directly correlated with the cooling rates of the molds: 1.2 °C/s for IC, 1.1 °C/s for NB, and 0.9 °C/s for SC. *PLA Removal:* The PLA model was successfully burned out without damaging the plaster shell, ensuring high geometric accuracy. *Final Output:* The combined IC and additive manufacturing process yielded high-quality bronze castings featuring 0.5% porosity, 95% equiaxed grains, and a controlled grain size of 25±2 μm.

*Scientific Novelty.* The research establishes a direct correlation between specific cooling rates of different mold types (IC, NB, SC) and the resulting microstructural and surface properties of bronze castings. Furthermore, it validates specific operational parameters—such as a 300 °C burnout temperature and precise geometric design allowances—for successfully integrating 3D-printed PLA models into the investment casting process to achieve highly uniform, defect-free bronze artworks.

**Key words:** Investment casting, artistic casting, bronze, 3D printing, 3D modeling.

**Гнатенко Михайло, Матвейшин Микита, Сергієнко Ольга, Іванов Валерій. Вплив типу форми на параметри якості поверхні та структуру при виготовленні художніх виливків із використанням моделей, отриманих адитивними методами**

*Мета дослідження.* Дослідити вплив різних формувальних матеріалів на якість поверхні та структурні характеристики бронзових, художніх виливків, а також оцінити технологічні переваги поєднання адитивного виробництва із процесом лиття за виплавлюваними моделями при виготовленні бронзових художніх виробів.

Методи дослідження. У дослідженні розглядали три методи лиття: лиття за випалюваними моделями у гіпсові форми (ЛВМ), лиття в самотвердіючі форми (СС) та лиття у піщано-глиняні форми (ПГС).

Майстер-модель: Для лиття в землю та СС застосовувалася неруйнівна модель, а для ЛВМ з PLA, модель видалляли при температурі 400 °C протягом години.

Проводився аналіз шорсткості поверхні ( $R_a$  і  $R_z$ ), розміру зерен, пористості та швидкостей охолодження форм.

Результати. Якість поверхні: Найкращі результати були отримані методом ЛВМ, що дозволило забезпечити найменшу шорсткість поверхні ( $R_a = 2.8$  мкм,  $R_z = 12.5$  мкм), найвищу точність передачі рельєфу, відсутність газової пористості та мінімальний пригар. Виливки, отримані ХТС, показали середній рівень якості поверхні, а піщано-глиняні – найгірший.

Дослідження мікроструктури проводилися шляхом визначення розміру зерна у поверхневій зоні виливків, для ЛВМ склав (25.3 мкм), для – СС (25.5 мкм) і ПГС (27.8 мкм).

Швидкість охолодження: Розмір зерен прямо корелював зі швидкістю охолодження форм: 1.2 °C/c для ЛВМ, 1.1 °C/c для СС і 0.9 °C/c для ПГС.

Видалення PLA-моделі: Модель успішно випалювалася без пошкодження керамічної оболонки, що забезпечило високу геометричну точність.

Кінцевий результат: Комбінація технологій ЛВМ та адитивного виробництва забезпечила високоякісні бронзові виливки з пористістю 0.5%, 95% рівновісних зерен і контрольованим розміром зерен  $25 \pm 2$  мкм.

Наукова новизна. Дослідження встановлює прямий зв'язок між певними швидкостями охолодження різних типів форм (ЛВМ, СС, піщано-глиняста) і відповідними мікроструктурними та поверхневими властивостями художніх, бронзових виливків. Крім того, підтверджено ефективність технологічних параметрів – таких як температура випалювання 400 °C і точні конструктивні припуски – для успішної інтеграції 3D-друкованих моделей з PLA у процес лиття за випалюваними моделями, що дозволяє отримати рівномірні, бездефектні бронзові мистецькі виливки.

**Ключові слова:** ЛВМ, Художнє лиття, лиття бронзи, 3D моделювання, 3D друк.

**Introduction.** Bronze alloys are among the most common materials in modern artistic casting and the production of awards and medals. Their popularity is due to their attractive appearance, good casting properties, and durability of the finished products [1; 2]. Artistic bronze products, such as sculptures, jewelry, commemorative medals, and award badges, are valued for their aesthetic and decorative qualities.

Bronze casting technologies are constantly evolving. Among modern methods, the most notable are investment casting using plaster shell molds and pressure die casting in metal molds [3]. These technologies ensure high surface quality and accurate reproduction of details in artistic products. However, their implementation is often limited by the cost of equipment and the complexity of mold manufacturing.

Along with progressive methods, traditional casting technologies using single-use sand molds remain in demand for artistic casting. In particular, sand-clay mixtures (SCM), cold-box sand mixtures (no-bake process), and plaster-based molds are widely used. The advantages of these methods include the availability of molding materials, the relative simplicity of mold production, and the ability to obtain castings with complex configurations and large sizes [4; 5].

**Research materials and methods.** The first stage of the research was to create a 3D model of the medal in the Rhinoceros (Rhino) 7.0 design system. Rhino was chosen as a convenient tool for modeling complex curved surfaces with the

possibility of subsequent printing on a 3D printer [9]. When developing the medal geometry, the specifics of the casting technology were taken into account. In particular, to facilitate the removal of the model from the mold, draft angles of at least 3° were provided on the vertical surfaces [10]. Special attention was paid to the formation of draft angles on small relief elements such as letters and patterns. The dimensions of the medal were chosen based on the manufacturability of casting and the requirements for the finished product: a diameter of 120 mm and a maximum thickness of 15 mm.

The 3D model created in Rhino was checked for the absence of geometry defects (surface discontinuities, self-intersections, etc.) that could interfere with quality printing or the formation of the casting mold. To evaluate the casting characteristics of the model, a computer simulation of metal pouring and solidification was carried out in the MagmaSoft system [11]. Based on the simulation results, minor adjustments were made to the geometry to prevent probable casting defects.

For the production of the master pattern, additive manufacturing technology was used, namely Fused Deposition Modeling (FDM). The FDM printing was performed on an Ultimaker 2+ 3D printer using PLA plastic with a layer thickness of 0.2 mm. This approach allows for the quick and cost-effective production of accurate master patterns for the subsequent manufacture of casting molds [12; 13]. The printed PLA model was processed and prepared for molding.



**Fig. 1. 3D model of the medal developed in Rhino and preparation for 3D printing in the slicer**

When creating the 3D model of the medal, special attention was paid to the formation of complex relief with fine elements (gear teeth, inscriptions, decorative symbols). This made it possible to assess the ability of different types of casting molds to reproduce fine surface details. Thus, the stage of 3D modeling and master pattern production is an important prerequisite for the successful casting of an artistic product. The use of modern CAD/CAM/CAE systems in combination with additive technologies allows optimizing the geometry of the cast part, anticipating and eliminating potential defects, and accelerating and reducing the cost of manufacturing a high-quality master pattern. To examine the influence of mold type on the surface quality of bronze castings, three mold variants were produced using the same master pattern: a sand-clay mold, a no-bake mold, and a plaster mold.

The sand-clay mold was prepared following conventional foundry practice from a molding mixture consisting of recycled molding clay, quartz sand, and water [14]. After compaction and drying, the mold surface was coated with a refractory wash based on kyanite–sillimanite.

The no-bake mold was manufactured from a mixture consisting of quartz sand with the addition of 1.5–2% phenol-formaldehyde resin (relative to the sand mass) and a catalyst in the amount of 15–20% of the resin mass. The components were homogenized in a paddle mixer until uniform distribution of the binder system was achieved. The prepared mixture was placed into the flask around the master pattern and compacted by vibration. To enhance the surface finish of the final casting, a graphite-based coating was applied onto the mold cavity surface [2].

To form the casting cavity in the block plaster mold, a hybrid pattern assembly was prepared. A gating and runner system, made of casting wax, was attached to the 3D-printed PLA master pattern. The use of low-melting-point wax for the gating system enables its complete evacuation during the initial dewaxing stage (Figure 2). This creates

unobstructed channels for gas venting during the subsequent high-temperature burnout (thermal degradation) of the polymer pattern.



**Fig. 2. Hybrid pattern assembly: a 3D-printed PLA master pattern with an attached wax gating system**

The plaster mold was produced from a mixture of construction gypsum, quartz sand, and water in a mass ratio of 1:2:0.7. Prior to molding, the master pattern surface was treated with a release agent; the sprue and risers were formed from modelling PLA and affixed to the pattern. The assembly was subsequently immersed layer by layer into the plaster slurry until a sufficient shell thickness was achieved. After setting, the Plaster investment mold was thermal burnout process at 700 °C for 1 hour to remove the PLA pattern, and then the mold was fired at 900–1000 °C to burn out PLA or organic materials and to develop the required strength.

Before metal pouring, the molds were preheated to 150–200 °C to remove residual moisture and improve the mold filling capability [15].

In summary, three mold systems differing in molding-mixture composition and fabrication technology were produced. This enables a comparative assessment of how these parameters affect the surface quality of artistic bronze castings.

**Results.** Visual inspection and profilometric measurements of the obtained castings revealed a significant difference in surface quality depending

on the type of mold used. The sample produced in the plaster mold exhibited a uniform metallic surface sheen and a minimal amount of burn-on. Fine relief elements such as gear teeth, font contours, and the boundaries of decorative symbols were reproduced with high fidelity. Profilo-metric analysis showed low roughness values: the arithmetic mean deviation of the profile  $Ra = 2.8 \mu\text{m}$ , the ten-point height of irregularities  $Rz = 12.5 \mu\text{m}$ , and the maximum profile height  $Rmax = 14 \mu\text{m}$ . According to visual evaluation, burn-on and gas porosity were practically absent (1 and 0 points out of 5, respective-ly), while relief sharpness received the maximum score (5/5).

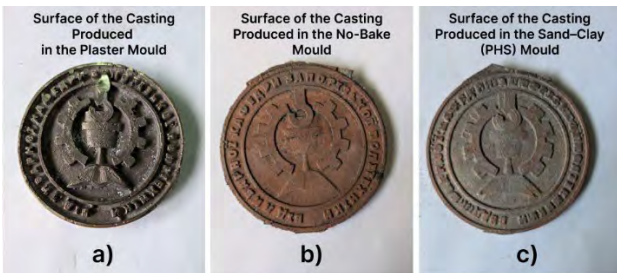


**Fig. 3. Comparison of the surface appearance of bronze castings produced in different mold types**

Metallographic analysis revealed a coarse-grained dendritic structure in the near-surface layers of the casting produced in the plaster investment mold, which can be attributed to the slow cooling and solidification processes [1; 2]. Such a structure may contribute to reduced plasticity and lower resistance to deformation [3]. It can be assumed that the low gas-forming tendency and high gas permeability of the plaster shell mold, along with its higher heat resistance and smooth cavity surface, ensured intimate contact with the melt without the formation of gas-related defects and minimized burn-on.

The casting obtained from the no-bake (CTS) mold exhibited slightly lower surface quality. Visual examination showed a uniform yet noticeable burn-on, and partial melting and rounding of relief edges were observed due to the thermal degradation of the resin binder. The surface roughness parameters were higher than those for the plaster mold:  $Ra = 5.4 \mu\text{m}$ ,  $Rz = 24 \mu\text{m}$ , and  $Rmax = 29 \mu\text{m}$ , corresponding to a burn-on rating of 2 points and a relief sharpness rating of 4 points out of 5. Gas porosity was evaluated at 1 point.

Metallographic analysis confirms that mold type decisively impacts bronze casting quality. While plaster molds yield the best surface finish with minimal defects, the no-bake mold showed acceptable intermediate results, exhibiting a slightly larger dendritic structure and minor surface burn-on due to resin gas

evolution and lower refractoriness. Conversely, the sand-clay mold proved completely unsuitable for precision artistic casting. Its high gas-forming tendency and low refractoriness led to a coarse dendritic structure, high porosity, and severe surface defects, including a coarse burn-on layer with up to a 30% loss of relief sharpness. It also recorded the highest roughness parameters ( $Ra = 10.6 \mu\text{m}$ ,  $Rz = 46 \mu\text{m}$ ,  $Rmax = 54 \mu\text{m}$ ) and the poorest visual scores (relief: 2/5, burn-on: 4/5), highlighting its inadequacy for precision applications.

Table 1

**Comparative Table of Surface Quality Indicators**

Indicator	Plaster	NoBake (CTS)	SandClay
Ra ( $\mu\text{m}$ )	2.8	5.4	10.6
Rz ( $\mu\text{m}$ )	12.5	24	46
Burn-on (1–5)	1	2	4
Gas porosity (1–5)	0	1	3
Relief sharpness (1–5)	5	4	2
Visual surface quality	High	Medium	Low

The obtained results are consistent with current understanding of the mechanisms governing casting surface formation and with literature data on the influence of mold type on defect formation [1–6]. The practical significance of this work lies in enabling a justified selection of molding materials and technologies for producing bronze artistic castings with predictable surface quality.

As can be seen, an increase in the thermal conductivity and grain size of the mold material leads to a corresponding rise in surface roughness:  $Ra$  increases from approximately  $2.8 \mu\text{m}$  (investment casting) to about  $10.6 \mu\text{m}$  (sand-clay mold), while  $Rz$  increases from  $12.5$  to  $46 \mu\text{m}$ . This confirms the significant influence of the molding material type on the surface quality of artistic bronze castings, even when using the same 3D-printed pattern for all three technologies.

A grid with a known spacing ( $25 \mu\text{m}$ ) was super-imposed on the metallographic images of the micro-structure. The number of intersections between grain boundaries and the grid lines was counted. Using equation (4.1), the average chord length of grain intercepts was calculated.

The mean grain size was determined using the intercept method.

The calculation was performed according to the formula:

$$d = \frac{M \cdot l}{n} \quad (1)$$

Where  $l$  is the total length of the test lines,  $M$  – is the magnification,  $N$  – is the number of intersections.

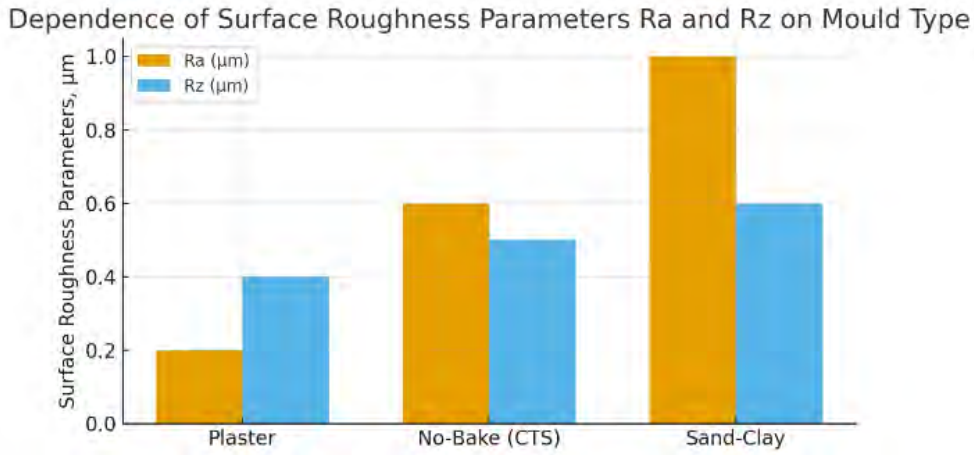


Fig. 4. Graph of the Dependence of Surface Roughness Parameters Ra and Rz on the Type of Mold

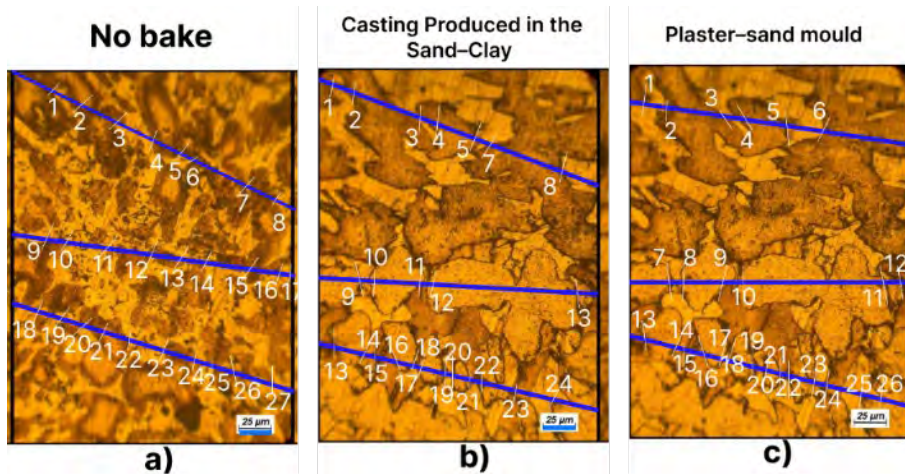


Fig. 5. Determination of the Average Grain Size

According to the obtained data, the smallest average grain size ( $25.3 \mu\text{m}$ ) is observed in the casting produced by investment casting (IC), which is associated with the slower cooling and solidification processes in the ceramic shell mold. The casting from the no-bake mold (NB) exhibits a slightly larger grain size ( $25.5 \mu\text{m}$ ), likely due to the exothermic reaction of the resin binder, which reduces the cooling rate. The largest grain size ( $27.8 \mu\text{m}$ ) was found in the casting produced in the sand-clay mold (SC), which is explained by the rapid cooling of the melt in contact with the mold material.

The obtained results correlate with the visual observations of the microstructure and confirm the assumed relationship between mold type and the crystallization behaviour of the metal.

The data presented in Table 2 demonstrates that the smallest average grain size ( $25.3 \mu\text{m}$ ) is observed in samples obtained by the Investment Casting (IC) method. This can be attributed to the

highest cooling and crystallization rates of the alloy in the thin-walled shell ceramic mold.

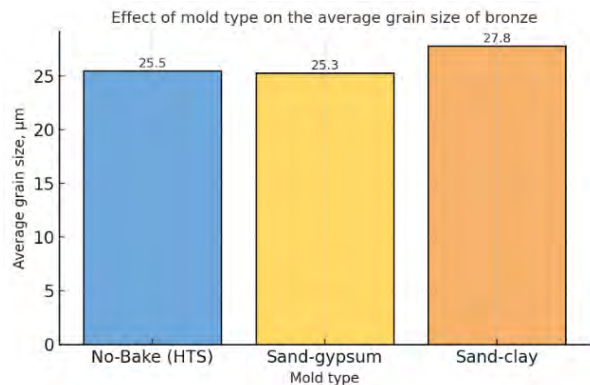


Fig 6. Dependence of Surface-Layer Grain Size on the Type of Mold

A slightly larger grain size ( $25.5 \mu\text{m}$ ) is characteristic of bronze obtained by casting in No-Bake (NB) molds. Evidently, the thermophysical

properties of the cold-hardening mixture provide a somewhat slower cooling of the melt compared to the plaster mold.

**Conclusions.** The selection of molding material decisively shapes both the surface integrity and microstructural features of bronze castings by regulating heat-transfer dynamics:

Investment Casting: Demonstrated the most favorable combination of properties. It yielded the finest, most uniform grain structure (25.3  $\mu\text{m}$ ) and exceptionally low surface roughness ( $R_a = 2.8 \mu\text{m}$ ,  $R_z = 12.5 \mu\text{m}$ ) with an almost complete absence of gas-related defects and precise relief reproduction.

No-Bake (NB/CTS) Molds: Provided acceptable surface quality and marginally coarser grains (25.5  $\mu\text{m}$ ) due to the thermophysical properties of the cold-hardening mixture, which somewhat slowed the cooling rate.

Sand-Clay Molds: Proved poorly suited for precision casting. Due to lower thermal conductivity

and unstable thermal behavior, they produced the largest grains (27.8  $\mu\text{m}$ ) alongside pronounced surface roughness, significant burn-on, and reduced geometric clarity.

A key practical achievement was the successful integration of a 3D-printed PLA master pattern into the investment casting workflow. The polymer was completely removed via burnout at 300 °C within 1 hour without compromising the mold, ensuring accurate reproduction of the designed geometry (including draft angles and technological allowances).

Summary: The synergy of additive manufacturing (3D printing) and investment casting is an optimal, cost-effective solution for unique or small-series artistic bronze production. It eliminates the need for expensive metal tooling, significantly reduces lead times, and ensures high-quality castings with complex geometries and superior structural control.

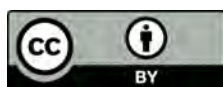
#### BIBLIOGRAPHY:

1. Nguyen T. T., Tran V. T., Nguyen V., Nguyen V. T. T. Effect of infill ratios in SLA 3D printing on mechanical properties of castable wax patterns for molded shells in investment casting. *PLOS ONE*. 2025. Vol. 20, No. 2. P. e0311245. DOI: <https://doi.org/10.1371/journal.pone.0311245>. (<https://doi.org/10.1371/journal.pone.0311245>)
2. Pelin G., Sonmez M., Pelin C.-E. The use of additive manufacturing techniques in the development of polymeric molds: a review. *Polymers*. 2024. Vol. 16, No. 8. P. 1055. DOI: <https://doi.org/10.3390/polym16081055>. (<https://doi.org/10.3390/polym16081055>)
3. Upadhyay T., Sivarupan T., El Mansori M. 3D printing for rapid sand casting – A review. *Journal of Manufacturing Processes*. 2017. Vol. 29. P. 211–220. DOI: <https://doi.org/10.1016/j.jmapro.2017.07.017>. (<https://doi.org/10.1016/j.jmapro.2017.07.017>)
4. Gnatenko M., Naumyk V., Matkovska M. Influence of sources of heating and protective gases on the properties of the material obtained by the direct deposition. *Materials Science and Technology 2019 (MS&T19) : contributed papers*. Portland, USA, 2019. P. 68–74.
5. Gnatenko M., Chigileichyk S., Sakhno S. Manufacture of aviation parts from heat-resistant nickel alloys by multilayer plasma surfacing. *Aerospace Technic and Technology*. 2021. No. 5 (175). P. 48–54. DOI: <https://doi.org/10.32620/akt.2021.5.06>. (<https://doi.org/10.32620/akt.2021.5.06>)
6. Abisuga O. A. et al. Study of investment casting process for 3D-printed design as an option for jewellery manufacturing. *MATEC Web of Conferences (RAPDASA 2022)*. 2022. Vol. 237. P. 04002. DOI: <https://doi.org/10.1051/mateconf/202237004002>. (<https://doi.org/10.1051/mateconf/202237004002>)
7. Bobby S. S., Singamneni S. Influence of moisture in the Gypsum molds made by 3D printing. *Procedia Engineering*. 2014. Vol. 97. P. 1618–1625. DOI: <https://doi.org/10.1016/j.proeng.2014.12.304>. (<https://doi.org/10.1016/j.proeng.2014.12.304>)
8. Espinoza-Cuadra J., Gallegos-Acevedo P., Mancha Molinar H., Pikado A. Effect of Sr and solidification conditions on characteristics of intermetallic in Al–Si 319 industrial alloys. *Materials and Design*. 2010. Vol. 31, No. 1. P. 343–356. DOI: <https://doi.org/10.1016/j.matdes.2009.01.045>. (<https://doi.org/10.1016/j.matdes.2009.01.045>)
9. Popielarski P., Ignaszak Z. Effective modelling of phenomena in over-moisture zone existing in porous sand mold subjected to thermal shock. *Drying and Energy Technologies. Advanced Structured Materials*. Cham : Springer, 2016. Vol. 63. P. 141–164. DOI: [https://doi.org/10.1007/978-3-319-19767-8\\_10](https://doi.org/10.1007/978-3-319-19767-8_10). ([https://doi.org/10.1007/978-3-319-19767-8\\_10](https://doi.org/10.1007/978-3-319-19767-8_10))
10. PN-EN 12524. Building materials and products. Hygrothermal properties – tabulated calculation values. EN 12524:2000. Brussels : CEN, 2000.
11. Biroş M. T., Ferenczy K., Andó M. Application of 3D printing in casting. *Mérnöki és Informatikai Megoldások / Engineering and Informatics Solutions II*. 2021. P. 4–13. DOI: <https://doi.org/10.37775/EIS.2021.2.1>. (<https://doi.org/10.37775/EIS.2021.2.1>)

12. Guler K. A., Çiğdem M. Casting quality of gypsum bonded block investment casting molds. *Advanced Materials Research*. 2012. Vol. 445. P. 349–354. DOI: <https://doi.org/10.4028/www.scientific.net/AMR.445.349>. (<https://doi.org/10.4028/www.scientific.net/AMR.445.349>)
13. Nedelcu D., Radu A., Stan S. Gypsum-bonded molds for casting of non-ferrous alloys: properties and microstructure. *Archives of Foundry Engineering*. 2021. Vol. 21, No. 2. P. 67–74. DOI: <https://doi.org/10.24425/afe.2021.136092>. (<https://doi.org/10.24425/afe.2021.136092>)
14. Lin Y.-C., Chen T.-C. et al. Influences of material selection, infill ratio, and layer height in the 3D printing cavity process on the surface roughness of printed patterns and casted products in investment casting. *Materials*. 2023. Vol. 16, No. 3. P. 941. DOI: <https://doi.org/10.3390/ma16030941>. (<https://doi.org/10.3390/ma16030941>)

#### REFERENCES:

1. Nguyen, T. T., Tran, V. T., Nguyen, V., & Nguyen, V. T. T. (2025). Effect of infill ratios in SLA 3D printing on mechanical properties of castable wax patterns for molded shells in investment casting. *PLOS ONE*, 20(2), e0311245. <https://doi.org/10.1371/journal.pone.0311245>
2. Pelin, G., Sonmez, M., & Pelin, C.-E. (2024). The use of additive manufacturing techniques in the development of polymeric molds: A review. *Polymers*, 16(8), 1055. <https://doi.org/10.3390/polym16081055>
3. Upadhyay, T., Sivarupan, T., & El Mansori, M. (2017). 3D printing for rapid sand casting – A review. *Journal of Manufacturing Processes*, 29, 211–220. <https://doi.org/10.1016/j.jmapro.2017.07.017>
4. Gnatenko, M., Naumyk, V., & Matkovska, M. (2019). Influence of sources of heating and protective gases on the properties of the material obtained by the direct deposition. In *Materials Science and Technology 2019 (MS&T19): Contributed papers* (pp. 68–74). Portland, OR.
5. Gnatenko, M., Chigileichyk, S., & Sakhno, S. (2021). Manufacture of aviation parts from heat-resistant nickel alloys by multilayer plasma surfacing. *Aerospace Technic and Technology*, 5(175), 48–54. <https://doi.org/10.32620/akt.2021.5.06>
6. Abisuga, O. A., Doran, K., & de Beer, D. (2022). Study of investment casting process for 3D-printed design as an option for jewellery manufacturing. *MATEC Web of Conferences*, 237, 04002. <https://doi.org/10.1051/mateconf/202237004002>
7. Bobby, S. S., & Singamneni, S. (2014). Influence of moisture in the Gypsum molds made by 3D printing. *Procedia Engineering*, 97, 1618–1625. <https://doi.org/10.1016/j.proeng.2014.12.304>
8. Espinoza-Cuadra, J., Gallegos-Acevedo, P., Mancha Molinar, H., & Pikado, A. (2010). Effect of Sr and solidification conditions on characteristics of intermetallic in Al–Si 319 industrial alloys. *Materials and Design*, 31(1), 343–356. <https://doi.org/10.1016/j.matdes.2009.01.045>
9. Popielarski, P., & Ignaszak, Z. (2016). Effective modelling of phenomena in over-moisture zone existing in porous sand mold subjected to thermal shock. In *Drying and energy technologies: Advanced structured materials* (Vol. 63, pp. 141–164). Springer, Cham. [https://doi.org/10.1007/978-3-319-19767-8\\_10](https://doi.org/10.1007/978-3-319-19767-8_10)
10. European Committee for Standardization. (2000). *Building materials and products - Hygrothermal properties - Tabulated calculation values* (EN 12524:2000). Brussels.
11. Biroş, M. T., Ferenczy, K., & Andó, M. (2021). Application of 3D printing in casting. *Mérnöki és Informatikai Megoldások / Engineering and Informatics Solutions II*, 4–13. <https://doi.org/10.37775/EIS.2021.2.1>
12. Guler, K. A., & Çiğdem, M. (2012). Casting quality of gypsum bonded block investment casting molds. *Advanced Materials Research*, 445, 349–354. <https://doi.org/10.4028/www.scientific.net/AMR.445.349>
13. Nedelcu, D., Radu, A., & Stan, S. (2021). Gypsum-bonded molds for casting of non-ferrous alloys: Properties and microstructure. *Archives of Foundry Engineering*, 21(2), 67–74. <https://doi.org/10.24425/afe.2021.136092>
14. Lin, Y.-C., Chen, T.-C., et al. (2023). Influences of material selection, infill ratio, and layer height in the 3D printing cavity process on the surface roughness of printed patterns and casted products in investment casting. *Materials*, 16(3), 941. <https://doi.org/10.3390/ma16030941>



Стаття поширюється на умовах  
ліцензії відкритого доступу  
CC BY 4.0

Дата першого надходження статті до видання: 09.04.2026  
Дата прийняття статті до друку після рецензування: 05.05.2026  
Дата публікації (оприлюднення) статті: 30.05.2026